CHAPTER FIVE

Solid-Like Domains in Mixed Lipid Bilayers: Effect of Membrane Lamellarity and Transition Pathway

Vernita D. Gordon[*,1,4], Paul A. Beales[*,2], Gemma C. Shearman[†,3], Zhijun Zhao[*], John M. Seddon[†], Wilson C.K. Poon[*], Stefan U. Egelhaaf[‡]

[*]SUPA, School of Physics, and Collaborative Optical Spectroscopy, Micromanipulation and Imaging Centre (COSMIC), The University of Edinburgh, Edinburgh, Scotland, United Kingdom
[†]Department of Chemistry, Imperial College London, South Kensington, London, United Kingdom
[‡]Condensed Matter Physics Laboratory, Heinrich-Heine-University, Düsseldorf, Germany
[1]Present Address: Department of Physics and Center for Nonlinear Dynamics, University of Texas at Austin, Austin, USA
[2]Present Address: Centre for Molecular Nanoscience, School of Chemistry, University of Leeds, Leeds LS2 9JT, United Kingdom
[3]Present Address: Molecular and Pharmaceutical Science, London Metropolitan University, London N7 8DB, United Kingdom
[4]Corresponding author: e-mail address: gordon@chaos.utexas.edu

Contents

Abstract

We present optical observations of phase separation in mixed model membranes in the form of giant unilamellar vesicles. These observations are compared to the phase behavior of lipid mixtures, which we determined by X-ray scattering and differential scanning calorimetry or extracted from the existing literature. The domain properties are affected

Advances in Planar Lipid Bilayers and Liposomes, Volume 20
ISSN 1554-4516
http://dx.doi.org/10.1016/B978-0-12-418698-9.00005-8

not only by the bulk phase behavior but also by the membrane lamellarity and phase transition pathways. These observations have important implications for how phase behavior determined by bulk methods using dense, *multilamellar* lipid bilayers are linked to phase separation in giant, *unilamellar* lipid bilayers as observed by microscopy.

1. INTRODUCTION

Complex patterns are often formed when multicomponent systems demix. Understanding these structures is a generic challenge across many areas of science. Among such systems are membranes formed by lipid mixtures. Lipids are essential constituents of biological membranes, in which demixing can produce heterogeneities vital to biological functions [1]. Lateral phase separation in mixed lipid bilayers leads to the formation of domains with distinct compositions, where the coexisting phases may be fluid or solid like. In the case of fluid-like domains, detailed theories relate the domain shape to the domains' elasticity and boundary properties [2,3]. In contrast, the understanding of solid-like domains is not as advanced. Our previous work using optical microscopy [4–6] suggests that the shape of micron-sized solid-like domains reflects the ordering of the lipids on a molecular level, which is determined by the specific solid phase constituting the domain. This is reminiscent of the way unit cell symmetries determine the shape of three-dimensional crystals [7].

However, the link from the behavior of two-dimensional unilamellar membranes to phase behavior has been based almost entirely on the structure and thermodynamics of *bulk* samples obtained using scattering techniques and calorimetry, respectively. The assumption that this procedure is valid has seldom been subjected to direct investigation. Such investigations are, for example, required for the design of patterned lipid membranes with particular domain textures for materials science purposes.

Here, we present such a study. We conduct scattering and calorimetric investigations of the phase behavior of several lipid mixtures in the bulk, and therefore necessarily multilamellar, state, and compare this work with our own and literature data obtained from the optical microscopy of domains in mixed unilamellar vesicles. We establish a correspondence between domain shape and phase structure, effects due to lamellarity [6] as well as non-equilibrium effects resulting from metastable phases. This understanding has important implications for interpreting lipid membrane studies and translating between investigations of *unilamellar* and *multilamellar* unsupported systems as well as supported and unsupported bilayers.

This study is based on model lipid systems. Freely suspended membranes in the form of giant unilamellar vesicles (GUVs) are important and widely used models for biological membranes [8]. Similar structures are also exploited in biotechnology as containers or delivery vectors [9]. Furthermore, it can be useful to first investigate the properties and behavior of model lipid systems and then seek to understand the behavior of more complex biological membranes.

2. MATERIALS AND METHODS

2.1. Preparation of vesicles

The following lipids were purchased from Avanti Polar Lipids and used without further purification: 1,2-dilauroyl-*sn*-glycero-3-phosphocholine (DLPC), 1,2-dimyristoyl-*sn*-glycero-3-phosphocholine (DMPC), 1,2-dipalmitoyl-*sn*-glycero-3-phosphocholine (DPPC), 1,2-distearoyl-*sn*-glycero-3-phosphocholine (DSPC), 1,2-diarachinoyl-*sn*-glycero-3-phosphocholine (DAPC), 1,2-dipalmitoyl-*sn*-glycero-3-phosphoethanolamine (DPPE), and 1,2-dipalmitoyl-*sn*-glycero-3-[phospho-L-serine] (sodium salt) (DPPS). These lipids were mixed in different molar ratios.

GUVs were prepared by electroformation. Chloroform solutions containing 0.50–0.67 mM lipids were dried in a nitrogen environment for at least 1 h before hydration and electroformation. Subsequently, standard electroformation techniques [10,11] were used to prepare GUVs with 10–50 μm diameter, as in previous experiments [4–6]. GUVs were formed at temperatures higher than the highest chain-melting temperature and the temperature then lowered with a cooling rate of typically 0.1–0.4 °C/min except where noted otherwise. Observations across a range of temperatures were done *in situ* with the vesicles adhering to each other and to the wire electrodes on which they were formed. Sites of intervesicle adhesion, or osculation, provide bilamellar regions to compare to unilamellar nonadhering regions.

For X-ray scattering and calorimetry, the lipid mixtures were lyophilized from chloroform solution. For each sample, the dry lipid was introduced into either a 1.5-mm glass capillary or pan for X-ray scattering and calorimetry, respectively, and an excess of HPLC grade H_2O (final water content 67 ± 1 wt%) added. At this lipid:water ratio, the sample is in the lamellar phase, with perhaps a few vesicles shed into the excess water. The sample was then sealed, centrifuged, and repeatedly temperature cycled, that is, frozen and then heated above its transition temperature, to remove any

inhomogeneity within the sample. The samples were subsequently stored at −5 °C until examination.

2.2. Optical microscopy

Phase separation in lipid membranes was visualized by confocal microscopy using trace amounts, total concentration 0.1–0.5 mol%, of preferentially partitioning amphiphilic fluorescent dyes (Molecular Probes): Lissamine rhodamine B 1,2-dihexadecanoyl-*sn*-glycero-3-phosphoethanolamine (Rh-DPPE), 2-(4,4-difluoro-5,7-dimethyl-4-bora-3a,4a-diaza-*s*-indacene-3-pentanoyl)-hexadecanoyl-*sn*-glycero-3-phosphocholine (BODIPY), 1,1′-dioctadecyl-3,3,3′,3′-tetramethylindocarbocyanine perchlorate (DiI-C-18), and 6-dodecanoyl-2-dimethylaminonaphthalene (Laurdan). No noticeable effects were observed upon changing the dyes, for example, substituting DiI-C-18 for Rh-DPPE or using only one dye at a time. This indicates that, at the present concentrations, the dyes have no significant effect on the observed behavior.

Images were acquired with an inverted Nikon microscope attached to a BIORAD confocal system. Images were processed and analyzed with the software ImageJ and IDL.

2.3. Wide-angle X-ray scattering

All wide-angle X-ray scattering (WAXS) measurements were performed in-house, using a low-power copper-target Bede Microsource (Durham, UK) X-ray generator with glass polycapillary optics. The quasi-parallel beam generated passed through a Ni filter and 300 μm pinholes, which resulted in a narrow beam of Cu K_α ($\lambda = 1.542$ Å) radiation. X-ray diffraction patterns were recorded using an intensified charge-coupled device "Gemstar" detector (Photonic Science, East Sussex, UK) and azimuthally averaged to give the scattered intensity I as a function of scattering vector $s = (2/\lambda)\sin(\theta/2)$ with θ the scattering angle. Samples were kept in 1.5-mm thin-wall glass capillaries and sealed before being introduced into the temperature-controlled sample holder. This allowed samples to be held at a constant temperature during study, to an accuracy of ±0.5 °C.

2.4. Differential scanning calorimetry

A Perkin-Elmer Diamond differential scanning calorimetry (DSC) was used for DSC measurements of DLPC:DPPC samples. Approximately 5–10 mg of the sample, the preparation of which was described earlier, was placed in

an aluminum pan that was then hermetically sealed. A reference pan was also prepared, containing approximately 20 mg of water. Both were heated from 5 to 80 °C and then cooled, at a constant rate of 5 °C/min. The temperature range was chosen to encompass the different chain-melting transitions of all lipid compositions investigated. This thermal cycle was repeated twice, and the third heating scan recorded, to ensure optimum reproducibility. Note that the DSC heating rate was significantly faster than the cooling rates employed in the microscopy experiments, in order to get sufficient thermal signal. The metastable effects seen in the microscopy samples are likely to cause only subtle thermal effects which would not be readily detectable in DSC scans from bulk samples.

3. RESULTS AND DISCUSSION

We present first an overview of the phase behavior and phase structure in our systems, based on our own work and the literature. We then draw a correlation between the shapes of micron-sized phase-separated domains observed by optical microscopy and the molecular-level characteristics of the phases that form them. This lays the foundation for us to explore the effects of two types of perturbation on our system. In the first, we discuss two examples of the transition pathway (i.e., the speed of the temperature quench) accessing *metastable* phases and how this is reflected in the phase-separated domains. In the second, we discuss how membrane *lamellarity* is coupled to domain formation, here in an equilibrium situation.

3.1. Phase behavior: Transition temperatures and structures

At high temperatures, unitary (single-component) bilayer membranes are in a quasi-2D fluid-like phase (L_α), in which the lipids have conformationally disordered hydrocarbon tails. Upon cooling below their melting temperature T_m, they can form various solid-like phases with ordered hydrocarbon tails (Fig. 5.1) [19]: The phosphoethanolamine (PE) and phosphoserine (PS) lipids studied here form a flat, untilted phase, L_β [12–14], with 2D hexagonal in-plane ordering of the hydrocarbon chains, for which, to our knowledge, no true long-range order has as yet been reported. The short- and medium-tail (12–16 carbons) phosphocholine (PC) lipids studied here form a solid-like phase, $P_{\beta'}$, with sawtooth ripples with a repeat distance of about 10 nm. Upon further cooling, these lipids form a flat, tilted phase, $L_{\beta'}$, with 2D near-hexagonal in-plane ordering that can extend over large areas [15,20].

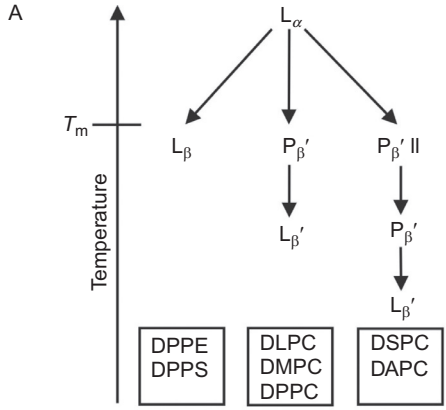

B

	L_β	$P_{\beta'}$	$P_{\beta'}$ II	$L_{\beta'}$
Dye in solid domains	L	L,D,R	L	–
Molecular order	Hexagonal	Hexagonal	Hexagonal	Hexagonal
Mesoscopic order	No order	Two fold (ripple)	Two fold (weak ripple)	Order
Observed shape				

Figure 5.1 (A) Schematic diagram of the phase behavior of single-component bilayer systems made of the lipids studied here [12–16]. (B) Summary of the relevant properties of the different solid phases: Dye partitionings into the solid-like domains (L, Laurdan; D, Di-I-C18; R, Rh-DPPE), microscopic and mesoscopic order reported in the literature [13,46,47], and shape of the domains we observe, which is compatible with shapes reported in the literature [17,18,48].

The long-tail (18 or 20 carbons) PC lipids studied here form a higher-temperature ripple phase, $P_{\beta'}$II, in which ripples are less steep and have a longer repeat distance than the usual $P_{\beta'}$ ripples; WAXS shows that lipids in $P_{\beta'}$II, have hexagonal in-plane ordering [16,21]. Upon further cooling, these bilayers form $P_{\beta'}$ and, at lower temperatures still, $L_{\beta'}$ phases [15].

For most of the binary lipid mixtures studied here, the phase behavior is well known [22–26], but in some cases, we have carried out our own determination in order to clarify specific issues: the liquidus line for DLPC:DPPC mixtures and the structure of DPPC:DPPS and DPPC:DPPE mixtures.

We determined the liquidus line for DLPC:DPPC mixtures using DSC (Fig. 5.2) and found the $P_{\beta'} - L_\alpha$ transition to occur at slightly higher temperatures than reported previously [26]. For example, we determined the liquidus

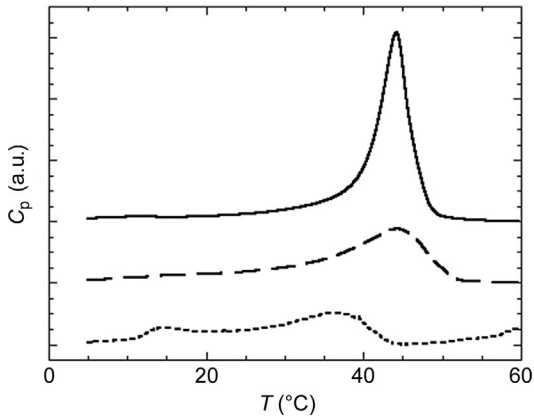

Figure 5.2 Typical differential scanning calorimetry (DSC) heating scans (5 °C/min) of DPPC:DLPC mixtures in excess water with molar ratios of 1:1, 3:1, and 9:1 (bottom to top). Shown is the excess heat capacity C_p as a function of temperature *T*. *Y*-axis in arbitrary units.

point for DLPC:DPPC 1:1 to be 37 °C, instead of 30 °C. Although the heating rate employed (5 °C/min) may have caused a small upward shift, this higher transition temperature is consistent with our microscopy observations at 33–34 °C of solid domains that are large enough to be optically resolved.

The $L_{\beta'}$ phase of pure DPPC in excess water has earlier been identified using WAXS, and the aliphatic chain tilt angle found to be approximately 30° [27]. Our WAXS data for pure DPPC at 25.0 °C show a somewhat broadened peak (at about 0.238 $Å^{-1}$) and shoulder (at about 0.244 $Å^{-1}$) (Fig. 5.3A) consistent with the previous results [27] and indicating the existence of an $L_{\beta'}$ phase. For DPPC:DPPS mixtures, with increasing DPPS fraction, the WAXS peak becomes more symmetrical, indicating that the cross-sectional chain-packing is approaching a regular hexagonal order. However, at a DPPC:DPPS ratio of 1:3 the peak is still slightly asymmetric, which may indicate a very slight tilt and the presence of an $L_{\beta'}$ phase. The asymmetry is more pronounced at lower temperatures, as indicated by the WAXS data at 37, 25, and 5 °C (Fig. 5.3B). Finally, for pure DPPS a single, sharper, gel peak is found, thus indicating the presence of an untilted L_β phase (Fig. 5.1), consistent with previous experiments [12].

We also used WAXS to investigate the phases formed by DPPC:DPPE mixtures at 25.0 °C (data not shown). These experiments indicate an $L_{\beta'}$ phase at high DPPC fractions, but no evidence of tilting was observed at a lower (25%) DPPC fraction, indicating the presence of an L_β phase. This is

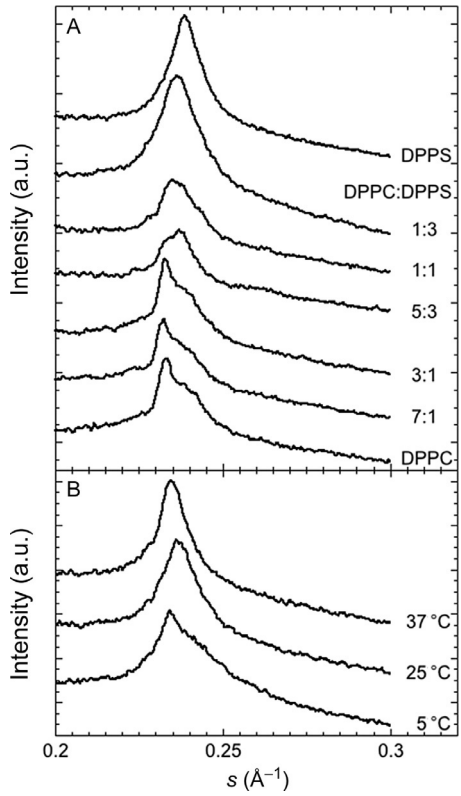

Figure 5.3 Wide-angle X-ray scattering (WAXS) intensity *I* as a function of scattering vector *s* for DPPC:DPPS mixtures in excess water (A) for different compositions at 25 °C and (B) for DPPC:DPPS 1:3 at different temperatures. *Y*-axis in arbitrary units.

in agreement with previous experiments which found an L_β phase for DPPC:DPPE mixtures with less than 50% DPPC, that is, a majority of DPPE [22].

3.2. Shape of solid-like domains

Mixtures of PC lipids with short and medium tails form a ripple phase, $P_{\beta'}$, upon cooling from the fluid phase (Fig. 5.1); the systems we observe are in the $L_\alpha - P_{\beta'}$ coexistence region [24,28]. For membranes of *short- and medium-tail PC lipids* (DLPC:DPPC and DMPC:DPPC) that are cooled below the liquidus line (see Section 3.1), we observe domains that exclude the dye BODIPY, a tail-modified lipid that has a bulky fluorophore in its hydrophobic region, and preferentially include the dyes Rh-DPPE and DiI-C-18 (Fig. 5.4). We have previously suggested [4] that these dyes are included because the large hydrophilic headgroups conferred by the

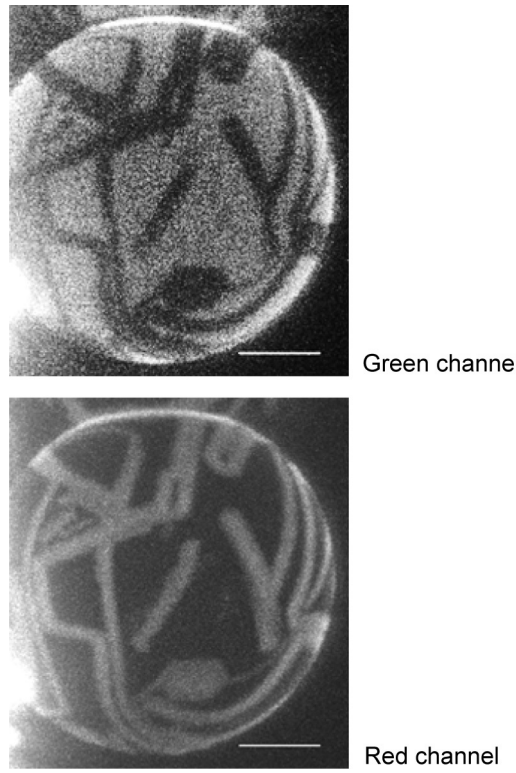

Figure 5.4 A DLPC:DPPC 1:3 vesicle at 36 °C. The domains exclude the dye BODIPY (green channel) and include the dye Rh-DPPE (red channel). Scale bar is 5 μm.

fluorophores are geometrically compatible with the extra free volume at the tops of the ripple crests. These domains are stripe-like, with high aspect ratio, and show preferred kinking at angles of 60° and 120° [4]. We have previously interpreted [4] the stripe-like shape, the quantized kinking, and the dye partitioning as resulting from the hexagonal lipid packing and the ripple sawtooth superstructure characteristic for a $P_{\beta'}$ phase.

For membranes containing *PC lipids with longer tails* (DLPC:DSPC, DMPC:DSPC, DLPC:DAPC), the first domains we see upon cooling grow where two unilamellar membranes adhere. They exclude BODIPY as well as Rh-DPPE and DiI-C-18 [6]. In DMPC:DSPC and DLPC:DAPC membranes, the domains are too small for their morphology to be resolved, while in DLPC:DSPC membranes domains can grow large enough for us to determine their shape; they are hexagonal with vertices always greater than 120° (Fig. 5.5). These solid-like domains are enriched in lipids that tend to form a

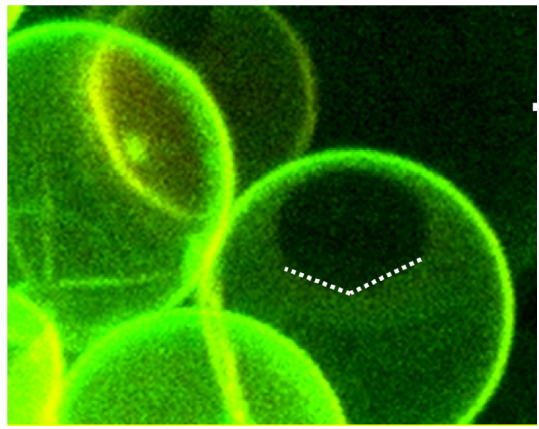

Figure 5.5 DLPC:DSPC 1:1 vesicles at 43 °C. The hexagonal domains grow where two unilamellar membranes adhere. Dotted lines are drawn along two edges of the hexagon as a guide to the eye. The domains exclude the dyes BODIPY and Rh-DPPE. Scale bar is 10 μm.

$P_{\beta'}$II phase (DSPC, DAPC) [16]. In mixed bilayers, the range of temperatures and compositions under which $P_{\beta'}$II exists is expected to be very limited for multilamellar systems, but can be extended for systems with lower lamellarity (see below). In $P_{\beta'}$II, the lipids are packed in a hexagonal symmetry. This is reflected in the hexagonal domain shape and vertices greater than 120°. An angle *greater* than 120° and the spherical shape of the vesicles indicate that the domains are curved similar to the surrounding fluid membrane. This is consistent with previous observations [17,29] and expected for a phase in which lipids have sufficient disorder to accommodate the packing defects required by a spherical surface [18,30]. Nonetheless, lipids are more ordered in $P_{\beta'}$II than in L_α. This ordering and the less pronounced superstructure of $P_{\beta'}$II compared to $P_{\beta'}$, explain the observed exclusion of dyes with bulky headgroups. Our observations are thus consistent with both the weak ripple structure of $P_{\beta'}$II and its formation at temperatures above $P_{\beta'}$ for unitary lipid systems [16,21] and with recent AFM results on a DMPC:DSPC mixture [31].

We also investigated mixtures containing *PS lipids* (DPPC:DPPS). Polygonal, often hexagonal, domains were found which exclude all the dyes we have tried (Fig. 5.6). Most vesicles had a low area fraction of the ordered phase and remained spherical, but we also observed a few nonspherical vesicles. According to the position of the solidus line in a previously published phase diagram, these domains are expected to have a DPPC:DPPS ratio of

about 1:3 [23] and according to our WAXS results are hence in the $L_{\beta'}$ phase. The long-ranged, hexagonal symmetry of the $L_{\beta'}$ is reflected in the hexagonal domain shape. Furthermore, the long-range and highly ordered $L_{\beta'}$ phase is likely to exclude impurities, such as dyes, consistent with our observations.

In mixtures containing *PE lipids* (DPPC:DPPE, DLPE:DPPE), the solid-like domains exclude all the dyes we have tried except Laurdan. They consist of circular units or subunits (Fig. 5.7) [4,5] with the same spherical curvature as the fluid regions. According to a previously published phase diagram and our own work, a DPPC:DPPE 1:1 mixture forms a L_{β} solid-like phase with about 75% DPPE upon cooling from the fluid phase (Fig. 5.1) [22]. Lipids in the L_{β} phase have significant rotational freedom [32]

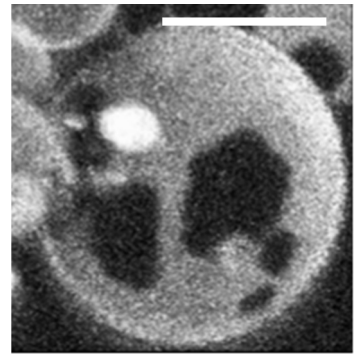

Figure 5.6 A DPPC:DPPS 3:1 vesicle at 40 °C. The domains exclude the dye Rh-DPPE. Scale bar is 10 μm.

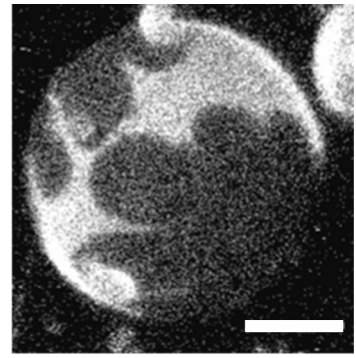

Figure 5.7 A DPPC:DPPE 1:1 vesicle at 45 °C. The domains exclude the dye Rh-DPPE. Scale bar is 10 μm.

and, to our knowledge, order over areas comparable to our domains has not been found. On the length scale of the domains, this phase is thus expected to be isotropic or multicrystalline. This absence of symmetry is reflected in the circular domain shape and consistent with the observed curvature of the solid-like domains. Furthermore, the L_β phase is locally flat which explains the observed dye exclusion.

3.2.1 Effect of transition pathway

Some domains have ramified shapes (Figs. 5.4, 5.6, and 5.7) which indicate incomplete coalescence. Hence the domain shapes do not necessarily minimize the system's energy and therefore are not controlled by thermodynamics, but rather by the kinetics of domain growth and rearrangements (in contrast to the situation with fluid domains) [2,3,33]. Rearrangements on the length scale of the domains take very long compared to our observation time (<24 h). The time for rearrangements is controlled by the lateral lipid diffusion, which in solid-like phases is very slow with diffusion coefficients $D \leq 10^{-11}$ cm^2/s [34–36]. These long structural relaxation times have further consequences. During cooling from the fluid phase into the fluid–solid coexistence region, the system may pass through nonequilibrium states. The dwell time in these states, which we control via the cooling rate, is also very short compared to structural relaxation times. We thus expect intermediate structures to affect the domain shapes.

We have previously observed such an effect for a mixture of *PC lipids with short and medium tails*, DLPC:DPPC, that forms a $L_{\beta'}$ phase after the temperature is lowered through $P_{\beta'}$ (Fig. 5.1) [4]. This system forms dye-containing stripes upon slow cooling (about 0.2 °C/min) from the fluid phase into the $P_{\beta'}$ phase (Fig. 5.4). However, faster quenches at about 0.8 °C/min frequently result in dye-containing hexagonal domains, with some of the hexagons having a dye-excluding center (Fig. 5.8). The hexagonal shape and its dye-free center are reminiscent of domains formed by $L_{\beta'}$ phase (Fig. 5.6). As previously explained [4], this happens because fast quenches can access the $L_{\beta'}$ at temperatures where it is metastable, before the system has time to phase separate and form domains of the equilibrium $P_{\beta'}$ phase. This is an example of the "Ostwald rule of stages" [37], by which a system may gradually decrease its free energy by going through a sequence of intermediate, metastable states [38]. The metastable $L_{\beta'}$ domains may template the growth of the $P_{\beta'}$ phase, giving rise to dye-containing hexagons. Alternatively, the metastable $L_{\beta'}$ domains may transform into $P_{\beta'}$ without

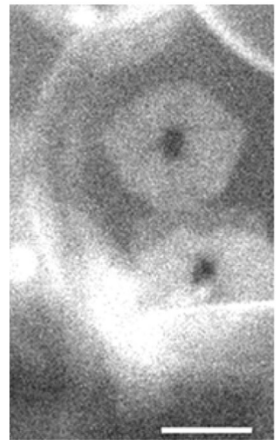

Figure 5.8 DLPC:DPPC 1:1 vesicles at 25 °C after rapid cooling (~0.8 °C/min). The domains exclude BODIPY (green channel) and preferentially include the dye Di-I-C18 (red channel). These hexagons sometimes have centers that are dark in both dyes. Scale bar is 4 μm.

significant mesoscopic morphological change because intradomain diffusion and thus rearrangements are slower than the $L_{\beta'} \rightarrow P_{\beta'}$ conversion [39,40]. Either scenario might explain the dye-containing hexagonal domains with dye-free centers that we observe.

Long-tail PC lipids can form an $P_{\beta'}$II phase as well as $P_{\beta'}$ and $L_{\beta'}$ phases (Fig. 5.1). Membranes containing a long-tail PC lipid (DLPC:DSPC, DMPC:DSPC) form dye-excluding, hexagonal domains under cooling rates of less than 0.2 °C/min (Fig. 5.5), which we attribute to the $P_{\beta'}$II phase. However, cooling at about 0.2 °C/min or faster produces stripe-like

domains [4]. At this faster cooling rate, stripes form even after initially hexagonal $P_{\beta'}$II domains have formed at a slower cooling rate. The cooling rate at which stripes appear depends on temperature; with decreasing cooling rates stripes appear at lower temperature until at about 0.1 °C/min stripes do not form even at room temperature [29]. From their shapes and dye partitioning, we attribute the stripe-like domains to the $P_{\beta'}$ phase. These observations indicate that in long-tail PC systems, $P_{\beta'}$II is the equilibrium phase for our compositions and temperatures and $P_{\beta'}$ is a metastable state accessible through rapid cooling. This is similar to the appearance of the $L_{\beta'}$ phase in the DLPC:DPPC system, except that in the long-tail PC systems no indication of a conversion from the metastable phase ($P_{\beta'}$) to the stable equilibrium phase ($P_{\beta'}$II) could be observed.

These experiments indicate that even if metastable intermediates have a short lifetime, intermediate structures may become kinetically trapped due to the very slow diffusion in solid-like phases. This leaves a long-lasting "fingerprint" of the transition pathway, which may be observable by microscopy.

3.2.2 Effect of membrane lamellarity

Bulk measurements show that the $P_{\beta'}$II phase exists for only a narrow temperature region in DSPC and not at all for DLPC [16,21,41]. Nevertheless, membranes composed of DLPC:DSPC 1:1, which should be far from the small region where $P_{\beta'}$II coexists with the fluid phase, form hexagonal, dye-excluding domains indicating a $P_{\beta'}$II phase (Fig. 5.5). We attribute this to the different membrane lamellarity. Decreasing lamellarity is expected to favor the fluid phase, L_α, and hence the free energy of unilamellar L_α is lower than the one of multilamellar L_α (Fig. 5.9) [6]. This decrease in free energy may shift the coexistence from $L_\alpha - P_{\beta'}$ (red dashed line) to $L_\alpha - P_{\beta'}$II (blue dash-dotted line) at fixed temperature and composition (vertical green dotted line), as shown by a common tangent construction [42]. In addition, we observe the hexagonal, dye-excluding domains across osculating bilayers. Again, lamellarity, but in this case local variations in lamellarity, affects the domains; solid domains prefer places with increased lamellarity, that is, osculating bilayers. This illustrates that lamellarity can affect the coexisting phases and hence the phase boundaries. Thus bulk, multilamellar systems and unilamellar (and low-lamellar) vesicles might have different phase behavior which in turn has implications for the domain shape and the location of the domains within the vesicles.

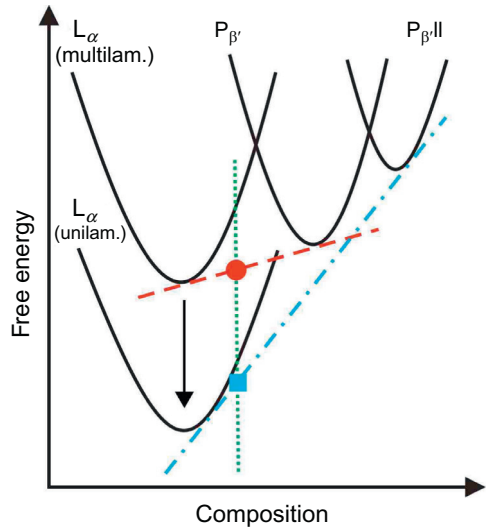

Figure 5.9 Possible schematic free-energy diagram for multi- and unilamellar L_α, $P_{\beta'}$, and $P_{\beta'}$II phases. As the lamellarity decreases (arrow), the free energy of the L_α phase decreases relative to the free energy of the other phases, which changes the coexistence from $L_\alpha - P_{\beta'}$ to $L_\alpha - P_{\beta'}$II as indicated by the common tangent construction.

4. SUMMARY AND OUTLOOK

We have studied model membranes in the form of GUVs composed of two saturated lipids with different hydrophobic chains and/or different hydrophilic headgroups. Lateral phase separation in the lipid bilayer causes solid-like domains to form in the otherwise fluid membrane. A previous conclusion [4] that the shape of these micron-sized domains reflects the ordering of the lipids on the molecular length scale has been found to hold also for the present pairs of lipids. The idea that domain shape is determined by the specific phase of the solid-like domains is therefore likely to be general.

When considering the phase behavior, based on which the domain shape is predicted or explained, membrane lamellarity has to be taken into account. We have shown that lamellarity affects the formation of solid-like domains (Fig. 5.5) [6]. With increasing lamellarity, membrane fluctuations are reduced and thus solid-like phases are preferred. This may change the phase behavior, which is typically determined for bulk, multilamellar samples. As a consequence, the domain morphology may also change. This finding is consistent with our previously-reported observation that adhesion of unilamellar GUVs induces and localizes phase separation [6].

Another point concerns metastable states, which might be visited during domain formation. The path followed during domain formation and growth, in particular the existence of intermediate, metastable states, can significantly affect the domain morphology. We varied the cooling rate and thus the dwell time in nonequilibrium states with respect to the structural relaxation times, which can be very long due to the slow diffusion in solid-like phases. We observed that the cooling rate can determine the domain shape (Figs. 5.4 and 5.8) [4]. That domain shapes in phase-separated systems can be kinetically determined is known for *bulk* materials (metals, synthetic, and biopolymers) [7]. What is intriguing here is our evidence for kinetic control on the *mesoscale* (microns) in GUVs—this is the length scale that makes them relevant as model systems for biological cells.

For cases where GUVs are relevant models for living cells, our findings contribute toward understanding heterogeneities in plasma membranes *in vivo*, for example, how these may be exploited in connection with membrane adhesion [43–45] and also with any membrane process, which necessarily involves nonequilibrium, intermediate states. Control of the process leading to domain formation allows living cells to manipulate the morphology of domains irrespective of the equilibrium conditions, such as composition or temperature. Beyond this, it allows us to exploit Ostwald's rule of stages and to design the process of domain formation, that is, include intermediate phases into the pathway, to control the resulting domain shape. Our findings may hence have implications for the rational design of patterned membranes, for example, for controlling the porosity and mechanical properties of vesicles as "smart" bio-delivery vehicles [9].

ACKNOWLEDGMENTS

We thank M. E. Cates, M. Deserno, J. Israelachvili, F. C. MacKintosh, J. Nagle, P. D. Olmsted, P. A. Janmey, M. Rappolt, M. Shipston, and R. H. Templer for stimulating and invaluable conversations. We thank A. Downie for constructing the electroformation chamber, J. Arlt and A. Garrie for technical support, and B. Moser for help with the diagrams. The work done in Edinburgh was funded by the EPSRC Grant GR/S10377 (Edinburgh Soft Matter and Statistical Physics Program Grant) and the work done at Imperial College London was funded by EPSRCs Platform Grant GR/S77721 and EP/G00465X.

REFERENCES

[1] D. Lingwood, K. Simons, Lipid rafts as a membrane-organizing principle, Science 327 (2010) 46–50.
[2] T. Baumgart, S.T. Hess, W.W. Webb, Imaging coexisting fluid domains in biomembrane models coupling curvature and line tension, Nature 425 (2003) 821–824.
[3] F. Jülicher, R. Lipowsky, Shape transformations of vesicles with intramembrane domains, Phys. Rev. E. 53 (1996) 2670–2683.

[4] V.D. Gordon, P.A. Beales, Z. Zhao, C. Blake, F.C. MacKintosh, P.D. Olmsted, M.E. Cates, S.U. Egelhaaf, W.C.K. Poon, Lipid organization and the morphology of solid-like domains in phase-separating binary lipid membranes, J. Phys. Condens. Matter 18 (2006) L415–L420.
[5] P. Beales, V. Gordon, Z. Zhao, S. Egelhaaf, W. Poon, Solid-like domains in fluid membranes, J. Phys. Condens. Matter 17 (2005) S3341.
[6] V. Gordon, M. Deserno, C. Andrew, S. Egelhaaf, W. Poon, Adhesion promotes phase separation in mixed-lipid membranes, Europhys. Lett. 84 (2008) 48003.
[7] A. Pimpinelli, J. Villain, Physics of Crystal Growth, Cambridge University Press, Cambridge, 1998.
[8] K. Simons, M.J. Gerl, Revitalizing membrane rafts: new tools and insights, Nat. Rev. Mol. Cell Biol. 11 (2010) 688–699.
[9] B.P. Timko, K. Whitehead, W. Gao, D.S. Kohane, O. Farokhzad, D. Anderson, R. Langer, Advances in drug delivery, Annu. Rev. Mater. Res. 41 (2011) 1–20.
[10] M.I. Angelova, D.S. Dimitrov, Liposome electroformation, Faraday Discuss. Chem. Soc. 81 (1986) 303–311.
[11] S. Manley, V.D. Gordon, Making giant unilamellar vesicles via hydration of a lipid film, Curr. Protoc. Cell Biol. (2008) (Chapter 24:Unit 24.3).
[12] R.N.A.H. Lewis, R.N. McElhaney, Calorimetric and spectroscopic studies of the thermotropic phase behavior of lipid bilayer model membranes composed of a homologous series of linear saturated phosphatidylserines, Biophys. J. 79 (2000) 2043–2055.
[13] H.I. Petrache, S. Tristram-Nagle, K. Gawrische, D. Harries, V.A. Parsegian, J.F. Nagle, Structure and fluctuations of charged phosphatidylserine bilayers in the absence of salt, Biophys. J. 86 (2004) 1574–1586.
[14] R. Koynova, M. Caffrey, Phases and phase transitions of the hydrated phosphatidylethaloamines, Chem. Phys. Lipids 69 (1994) 1–34.
[15] R. Koynova, M. Caffrey, Phases and phase transitions of the phosphatidylcholines, Biochim. Biophys. Acta 1376 (1998) 91–145.
[16] K. Jorgensen, Calorimetric detection of a sub-main transition in long-chain phosphatidylcholine lipid bilayers, Biochim. Biophys. Acta 1240 (1995) 111–114.
[17] L.A. Bagatolli, E. Gratton, Two photon fluorescence microscopy of coexisting lipid domains in giant unilamellar vesicles of binary phospholipid mixtures, Biophys. J. 78 (2000) 290–305.
[18] A.R. Bausch, M.J. Bowick, A. Cacciuto, A.D. Dinsmore, M.F. Hsu, D.R. Nelson, M.G. Nikolaides, A. Travesset, D.A. Weitz, Grain boundary scars and spherical crystallography, Science 299 (2003) 1716–1718.
[19] V. Luzzati, A. Tardieu, Lipid phases: structure and structural transitions, Annu. Rev. Phys. Chem. 25 (1974) 79–94.
[20] D. Rüppel, E. Sackmann, On defects in different phases of two-dimensional lipid bilayers, J. Phys. 44 (1983) 1025–1034.
[21] K. Pressl, K. Jorgensen, P. Laggner, Characterization of the sub-main-transition in distearoylphosphatidylcholine studied by simultaneous small- and wide-angle X-ray diffraction, Biochim. Biophys. Acta 1325 (1997) 1–7.
[22] A. Blume, R.J. Wittebort, S.K. Das Gupta, R.G. Griffin, Phase equilibria, molecular conformation, and dynamics in phosphatidylcholine/phosphatidylethanolamine bilayers, Biochemistry 21 (1982) 6243–6253.
[23] E.J. Luna, H.M. McConnell, Lateral phase separations in binary mixtures of phospholipids having different charges and different crystalline structures, Biochim. Biophys. Acta 470 (1977) 303–316.
[24] E.J. Luna, H.M. McConnell, Multiple phase equilibria in binary mixtures of phospholipids, Biochim. Biophys. Acta 509 (1978) 462–473.
[25] S. Mabrey, J.M. Sturtevant, Investigation of phase transitions of lipids and lipid mixtures by high sensitivity differential scanning calorimetry, Proc. Natl. Acad. Sci. U. S. A. 73 (1976) 3862–3866.

[26] P.W.M. van Dijck, A.J. Kaper, H.A.J. Oonk, J. de Gier, Miscibility properties of binary phosphatidylcholine mixtures: a calorimetric study, Biochim. Biophys. Acta 470 (1977) 58–69.
[27] M.J. Ruocco, G.G. Shipley, Characterization of the sub-transition of hydrated dipalmitoylphosphatidylcholine bilayers, Biochim. Biophys. Acta 691 (1982) 309–320.
[28] T. Kaasgaard, C. Leidy, J.H. Crowe, O.G. Mouritsen, K. Jorgensen, Temperature-controlled structure and kinetics of ripple phases in one- and two-component supported lipid bilayers, Biophys. J. 85 (2003) 350–360.
[29] L.A. Bagatolli, E. Gratton, A correlation between lipid domain shape and binary phospholipid mixture composition in free standing bilayers: a two-photon fluorescence microscopy study, Biophys. J. 79 (2000) 434–447.
[30] Y. Chushak, A. Travesset, Solid domains in lipid vesicles and scars, Europhys. Lett. 72 (2005) 767–773.
[31] M.-C. Giocondi, C. Le Grimellec, Temperature dependence of the surface topography in dimyristoylphosphatidylcholine/distearoylphosphatidylcholine multibilayers, Biophys. J. 86 (2004) 2218–2230.
[32] A. Blume, D.M. Rice, R.J. Wittebort, R.G. Griffin, Molecular dynamics and conformation in the gel and liquid-crystalline phases of phosphatidylethanolamine bilayers, Biochemistry 21 (1982) 6220–6230.
[33] R. Lipowsky, R. Dimova, Domains in membranes and vesicles, J. Phys. Condens. Matter 15 (2003) S31.
[34] P.F.F. Almeida, W.L.C. Vaz, T.E. Thompson, Lateral diffusion and percolation in 2-phase, 2-component lipid bilayers - topology of the solid-phase domains in-plane and across the lipid bilayer, Biochemistry 31 (1992) 7198–7210.
[35] A.E. Hac, H.M. Seegers, M. Fidorra, T. Heimburg, Diffusion in two-component lipid membranes—a fluorescence correlation spectroscopy and Monte Carlo simulation study, Biophys. J. 88 (2005) 317–333.
[36] M.J. Saxton, Lateral diffusion of lipids and proteins, Curr. Top. Membr. 48 (1999) 229–282.
[37] W. Ostwald, Studien über die Bildung und Umwandlung fester Körper, Z. Phys. Chem. 22 (1897) 289–330.
[38] V.J. Anderson, H.N.W. Lekkerkerker, Insights into phase transition kinetics from colloid science, Nature 416 (2002) 811–815.
[39] M.B. Schneider, W.K. Chan, W.W. Webb, Fast diffusion along defects and corrugations in phospholipid Pβ' liquid crystals, Biophys. J. 43 (1983) 157–165.
[40] P. Laggner, M. Kriechbaum, G. Rapp, Structural intermediates in phospholipid phase transitions, J. Appl. Crystallogr. 24 (1991) 836–842.
[41] M. Nielsen, L. Miao, J.H. Ipsen, K. Jorgensen, M.J. Zuckermann, O.G. Mouritsen, Model of a sub-main transition in phospholipid bilayers, Biochim. Biophys. Acta 1283 (1996) 170–176.
[42] R.T. Dehoff, Thermodynamics in Materials Science, McGraw-Hill, Inc., London, 1993.
[43] M.A. Barocchi, V. Masignani, R. Rappuoli, Cell entry machines: a common theme in nature? Nat. Rev. Microbiol. 3 (2005) 349–358.
[44] E.H. Chen, E.N. Olson, Unveiling the mechanisms of cell-cell fusion, Science 308 (2005) 369–373.
[45] J.S. Bonifacino, B.S. Glick, The mechanisms of vesicle budding and fusion, Cell 116 (2004) 153–156.
[46] J. Katsaras, S. Tristram-Nagle, Y. Liu, R.L. Headrick, E. Fontes, P.C. Mason, J.F. Nagle, Clarification of the ripple phase of lecithin bilayers using fully hydrated, aligned samples, Phys. Rev. E Stat. Phys. Plasmas Fluids Relat. Interdiscip. Topics 61 (2000) 5668–5677.
[47] W.J. Sun, S. Tristram-Nagle, R.M. Suter, J.F. Nagle, Structure of gel phase saturated lecithin bilayers: temperature and chain length dependence, Biophys. J. 71 (1996) 885–891.
[48] J. Korlach, P. Schwille, W.W. Webb, G. Feigenson, Characterization of lipid bilayer phases by confocal microscopy and fluorescence correlation spectroscopy, Proc. Nat. Acad. Sci. U. S. A. 96 (1999) 8461–8466.